



Pediatric Retinal Research Laboratory  
Eye Research Institute  
Oakland University  
Rochester Michigan, USA



## Longitudinal Validation Study: Image Guided Focal ERG Analysis in a Mouse Oxygen Induced Retinopathy Model of Ischemia

K.P. Mitton<sup>1</sup>, S.C. Wong<sup>1</sup>, K. Drenser<sup>1,2</sup>, E. Guzman<sup>1</sup>, M. Cheng<sup>1</sup>, W. Dailey<sup>1</sup>, M. Trese<sup>1,2</sup>

1Eye Research Institute - Pediatric Retinal Research Lab, Oakland University, Rochester, MI  
2Vitreous Retinal Surgery, Associated Retinal Consultants, Novi, MI. ABSTRACT

Mouse models of Human retinal diseases continue to be developed to support molecular investigations and therapeutic development. We tested the capability of the novel ERG / image-guided Micron-III System (Phoenix Research Labs) to obtain focal ERG data from discrete areas of the murine retina, using an oxygen induced retinopathy model, to monitor A-wave and B-wave changes in regions small enough to have uniform effects. These regions were monitored longitudinally in the same eye of the same animals over several weeks. Work began with a prototype and data for this paper were obtained with a final version of the Focal ERG module, with a gold corneal electrode integrated into the ocular lens mount. Dark-adapted B6.Cg-TgThy1-YFP mice, which express YFP in ganglion cells, were anesthetized after dilation of pupils. Continuous LED illumination in the red spectrum, and real time video imaging, was used to locate the disc and then target discrete retinal zones. LED illumination was switched to white light and pulse mode for control of ERG acquisition using the Micron-III ERG controller (Phoenix Research Labs). A robust dark-adapted ERG response with characteristic A-wave, B-wave, and oscillatory potentials was obtained with illumination zones as small as the murine disc. Focal ERG in the murine eye is efficient with the Micron-III system as tested. Using a temperature control pad, Focal-ERG and fluorescein angiography could be completed on the same eye before the formation of transient lens opacities. Targets are small enough to isolate the ERG response from control and treated regions of the same eye, or to test degenerations in different retinal zones. Live imaging capability makes targeting certain and provides a visual record of the ERG testing, which should be very useful for documentation during therapeutic testing. In the case of the OIR mouse model, the Focal-ERG system demonstrated clearly for the first time, that the B-wave is at first lost completely before it recovers to about 50% of normal after neovascularization. Photoreceptors remain responsive at all times, without loss of the A-wave.

(Information in this report was presented at the ARVO-ISIE meeting, May 5<sup>th</sup>, 2012. Ft Lauderdale.)

### INTRODUCTION

Mouse models of retinal diseases; include strains with naturally occurring mutations (rd1, rd7) or those engineered with transgenic technology (transgenes, knockouts, knockins, conditional knockouts) (1, 2). These models continue to reveal the roles of transcription factors

in retinal development, as well as the function of gene products in microvascular development, photo-transduction, intracellular trafficking, outer-segment formation, and synaptogenesis. All of these processes are implicated in retinal degeneration mice and in Human retinal dystrophies. In various Human retinal diseases, the initial pathology and the progress of retinal changes are rarely uniform throughout the entire retina area. There are often profound differences in both the radial direction and distance from the disc, or between the central and peripheral retina.

While the Human retina is routinely monitored with non-invasive testing to compare different zones, the mouse eye requires optical systems for working through a dilated pupil of only 0.9 mm in diameter. Useful disease research models, such as the oxygen induced retinopathy (OIR) model, and testing with sub-retinal injections (genes/cells) would benefit from the ability to compare different retinal areas within the same eye (3-6). We demonstrate here how non-invasive retinal imaging, combined with focal-ERG, can explore the relationships between neural function, the microvasculature, and cell distributions in an Oxygen Induced Retinopathy model.

Full field ERG analysis has previously demonstrated an average reduction in the ERG B-wave amplitude, consistent with the loss of bipolar cells (7). These morphological changes are not homogenous throughout the retinas of OIR mice and thus the question remained: is the photoreceptor A-wave response altered or unchanged in homogenous zones of diminished B-wave response? Through the use of LED light stimulation targeting areas just larger than the murine disc, we were able to answer this question with certainty.

## **METHODS and RESULTS**

*Animals* - This study was approved by the Oakland University IACUC and complied with the ARVO Statement for the Use of Animals in Ophthalmic and Vision Research. Mice expressing YFP in a subset of ganglion cells (B6.Cg-Tg(Thy1-YFP)HJrs/J) were obtained from JAX Labs.

*Oxygen-induced Retinopathy*- Pre-weanling litters were housed in 75% oxygen for five days, as per Smith et al. (1993), from P7 to P12 (not P0 to P5). Litters were then returned to room air. This exposure window was late enough to minimize dilation effects on the regressing hyaloid vessels, and early enough to overlap with retinal vascular development. A maximal neovascularization response occurs in this model between age P17 and P21.

*Micron-III system imaging and Focal-ERG* - We adopted the Micron-III for digital imaging, and the Focal-ERG attachment for this system starting with a prototype (Greg Sprehn, Phoenix Research Labs) and then the currently available unit, used for data presented here (**Fig-1**). To permit an analysis time of 30 minutes per animal, mice were anesthetized with 50

mg/kg Ketamine HCl, and 7 mg/kg Xylazine, delivered IP injection in PBS.

Before anesthesia, pupils were dilated with Tropicamide and Phenyephrine eye drops, both delivered twice, 5 minutes apart. This ensured maximum dilation prior to anesthesia. Once the blinking reflex was halted, corneas were kept moist with hypromellose solution (for example Goniovisc brand). This solution also provided optical coupling to the ERG lens of the focal ERG attachment, and provided low impedance for electrical coupling to the lens' mount which also served as the measuring electrode (gold). A mouse support included a thermal heating pad set for 37°C, which was necessary to avoid temperature loss under anesthesia, which significantly reduces the ERG response and speeds the onset of transient lens opacity.

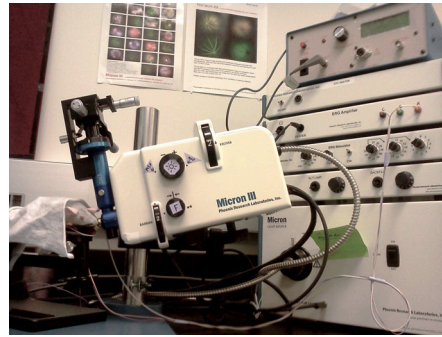
**Figure 1. Micron-III System, Pediatric Retinal Research Lab, Eye Research Institute, Oakland University.**

**A)** Micron-III bench layout. **B)** Camera with focal ERG attachment and stack, from bottom: camera power/light, slit-lamp controls, focal-ERG flash control/trigger, focal-ERG amplifier interface/heater, additional heating, temperature monitor. **C)** Focal-ERG targeting controls. **D)** Mouse warming support.

**A**



**B**



**C**

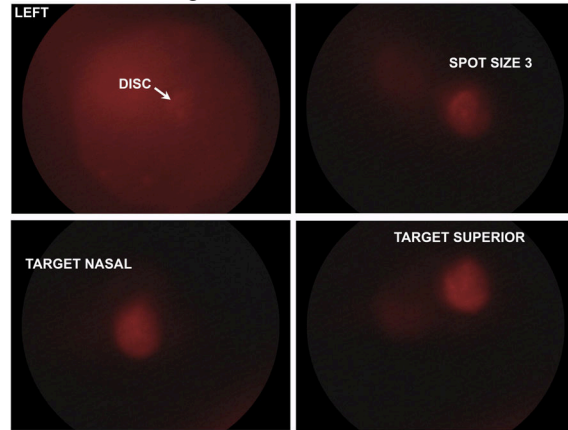


**D**



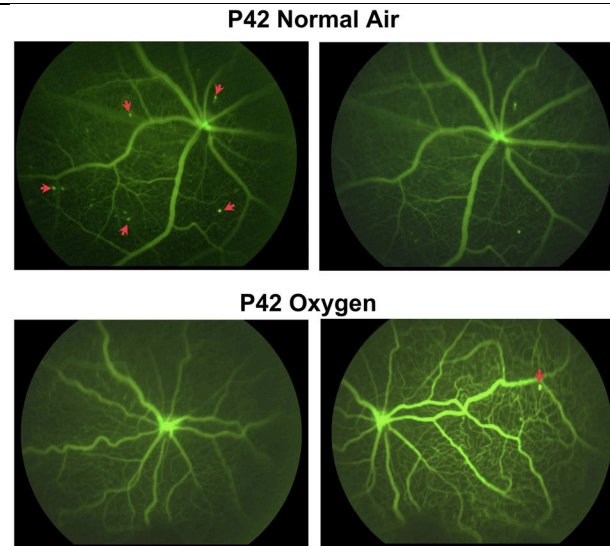
We obtained focal-ERG data from small target areas (**Fig-2**) and imaging data (YFP ganglion cell imaging, fluorescein angiography) from the same eyes within 30 minutes (**Fig-3**) under Ketamine-Xylazine anesthesia. A red filter on the Focal-ERG's LED light source was used to just enable visualization of the disc in mice after 1.5 hours of dark adaptation. **Figure-2** illustrates the initial identification of the disc in an eye (left eye). The same spot was then decreased in size, in this case spot size selection of 3. (Spot size 10 was about the size of the entire visual field. Size 3 was just about as small as the disc itself. This target size was used in continuous red-light mode to move to the desired target region, relative to the disc. Then ERG recordings were obtained in regions just adjacent to the disc in the order: temporal, nasal, superior and inferior.

**Fig 2. Focal ERG Targeting.** Images were obtained during acquisition of the P42 Oxygen focal-ERG data shown in Fig-4.



The optics of the Micron-III ERG lens are coupled with the physiological optics of the mouse eye, thus directions are not reversed during viewing. i.e. Up is up and left temporal is to the right of the disc as viewed on the monitor. **Figure-2** illustrates the nasal and superior target positions. The same mice could be followed over several weeks, using the oxygen-induced retinopathy model. Because of the targeting scheme chosen, the same regions could also be re-tested each week. Furthermore, and most importantly, the spot size for illumination was small enough to test a zone with homogenous local morphology.

**Fig 3. Post-ERG Imaging: Fluorescein Angiography and Ganglion Cells (YFP).** GC's are visible (red arrows) prior to fluorescein injection using the standard fluorescein filters. Images were captured using the Micron-III's main light through the focal-ERG lens, immediately after collecting focal-ERG data. Note the torturous vessel morphology in the OIR retina after neovascularization.



We obtained focal-ERG data from small target areas (**Fig-2**) and imaging data (YFP ganglion cell imaging, fluorescein angiography) from the same eyes within the same 30 minutes (**Fig-3**). The strain used here, had endogenous expression of the YFP protein in a subset of ganglion cells in the neural retina. Prior to the injection of fluorescein, these cells could be viewed using the Micron-III standard fluorescein filter set or a custom set of filters that gives maximum sensitivity for YFP. The later set was used mostly with the standard Micron-III mouse lens for detailed imaging of ganglion cell dendrites. Here, for Focal-ERG, we have imaged the retina using the Focal-ERG's integrated lens. (Fig-3)

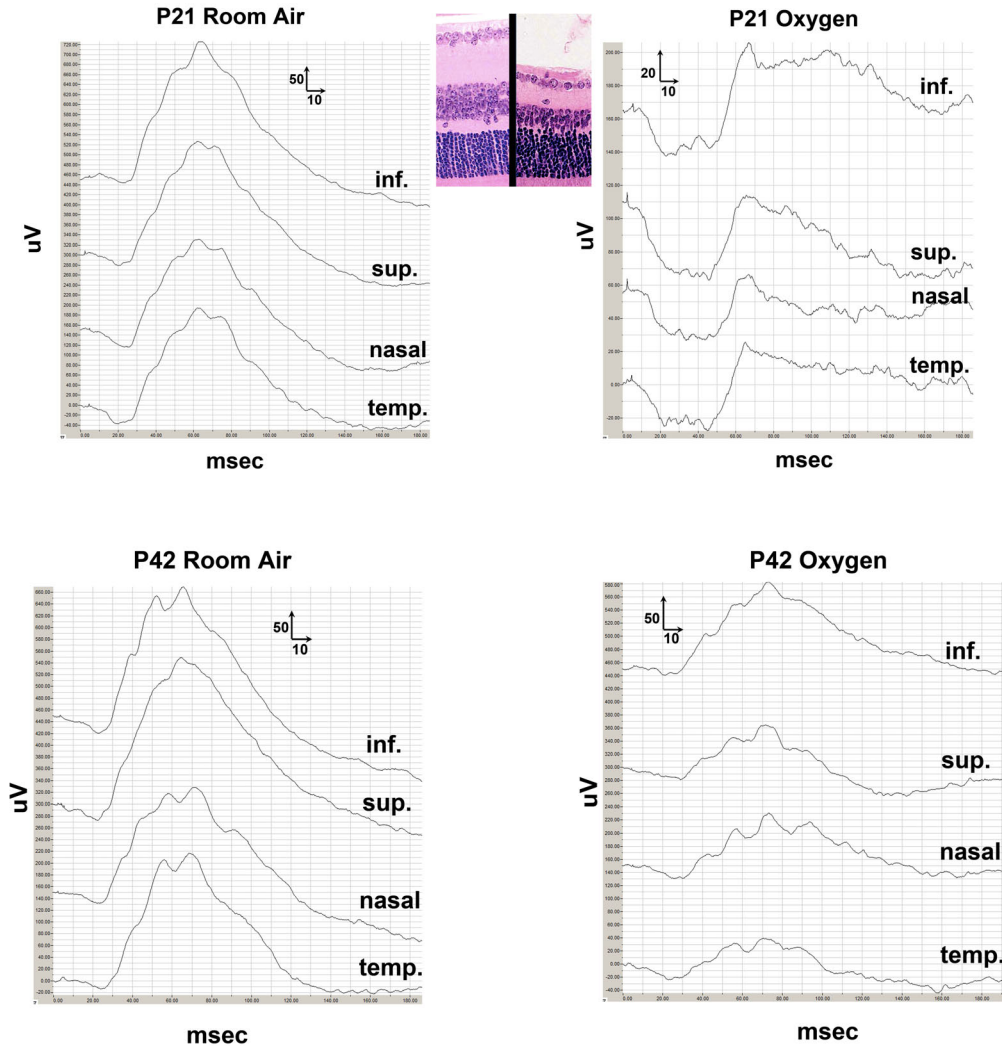
YFP ganglion cells are indicated, and two shifted views of the same retina are shown for both a P42 control (normal air) and P42 oxygen treated mouse. Please note that the P42 oxygen retina in **Figure-3** is the same retina for which we have presented ERG data in **Figure-4**. Both the A-Wave and B-Wave response were monitored from small areas and the ERG traces are shown in **Figure-4** for P21 and P42. Oxygen treated and age matched room air control mice are compared. Not the loss of bipolar cells characteristic of this model, already seen clearly at age P21 (**Fig-4** inset). Using the procedures we have developed, it was possible to obtain excellent familiar ERG traces from even this very small portion of the murine retina, the size of the disc.

For ERG acquisition, the LED light source was switched from continuous illumination to trigger mode, and the light filter dial changed to white light. Each ERG trace was averaged from 20 collections using a 30 msec flash duration and maximum LED intensity setting of 30. (Raw Lux output to sensor is 8560 with spot diameter setting of 5. Greg Sprehn.) ERGs were captured in the order: temporal, nasal, superior, inferior. All four locations could be completed in about 5 minutes.

Results in **Figure-4** clearly showed that the A-wave response of the photoreceptor layer mostly remains intact, consistent with the morphology of OIR retinas as used in our hands. The photoreceptor outer nuclear layer maintains a normal thickness, and inner and outer segments remain. However, consistent with the loss of bipolar cells, the B-wave is dramatically lost by age P21. At this time neovascularization is nearing completion. Surprisingly, the Focal-ERG technique also revealed that the B-wave is lost and then actually recovers substantially by age P42.

Thus, the loss of the B-wave at P21 is not just reflecting the loss of bipolar cells but also a temporary impairment of the ischemic retina that seems to recover some B-wave activity within two more weeks after P21.

**Fig 4. Partial Recovery of the B-Wave in an OIR Model.** Room air and oxygen treated controls were tested at ages P21 and P42. Targets were around the disc. Note the severe loss of the B-wave by P21, while the photoreceptor-derived A-wave was present. Focal-ERG of the same OIR retina, showed a progressive recovery of the B-Wave to about 50% of control by P42. Partial recovery was consistent with the permanent loss of bipolar cells. Test conditions: dark adapted, LED white illumination, intensity 30 (mixed rod/cone), average 20 flashes (30 msec), LabScribe software with the Phoenix ERG module.



## CONCLUSIONS

- 1. The Micron-III focal-ERG provided reproducible image-guided targeting of small retinal areas.**
- 2. Photoreceptor cells remained functional in the murine OIR model, even when the B-wave was absent. Partial recovery of lost retinal function, downstream of the photoreceptors, occurred with revascularization.**
- 3. Focal-ERG, fluorescein angiography, and imaging of fluorescent ganglion cells were possible in a single session of anesthesia.**

Research Support: ROPARD (Virginia and Clarence Clohset estate), Lincy Foundation, OU-CBR.

## References

1. Bowes C, Li T, Danciger M, Baxter LC, Applebury ML, Farber DB. Retinal degeneration in the rd mouse is caused by a defect in the beta subunit of rod cGMP-phosphodiesterase. *Nature*. 1990;347(6294):677-80.
2. Chang B, Hawes NL, Hurd RE, Davisson MT, Nusinowitz S, Heckenlively JR. Retinal degeneration mutants in the mouse. *Vision Res*. 2002;42(4):517-25.
3. Gole GA, Browning J, Elts SM. The mouse model of oxygen-induced retinopathy: a suitable animal model for angiogenesis research. *Documenta ophthalmologica Advances in ophthalmology*. 1990;74(3):163-9.
4. Ricci B. Oxygen-induced retinopathy in the rat model. *Documenta ophthalmologica Advances in ophthalmology*. 1990;74(3):171-7.
5. Smith LE, Wesolowski E, McLellan A, Kostyk SK, D'Amato R, Sullivan R, et al. Oxygen-induced retinopathy in the mouse. *Investigative ophthalmology & visual science*. 1994;35(1):101-11.
6. Krohne TU, Westenskow PD, Kurihara T, Friedlander DF, Lehmann M, Dorsey AL, et al. Generation of retinal pigment epithelial cells from small molecules and OCT4-reprogrammed human induced pluripotent stem cells. *Paediatr Int Child Health*. 2012;1(2):96-109. PMID: 3328503.
7. Nakamura S, Imai S, Ogishima H, Tsuruma K, Shimazawa M, Hara H. Morphological and functional changes in the retina after chronic oxygen-induced retinopathy. *PloS one*. 2012;7(2):e32167. PMID: 3279421.

*(Copywrite 2012 Mitton, Wong, Drenser, Guzman, Cheng, Dailey, Trese. Not to be reproduced without permission.)*